Article

Structural design optimization and vibration assessment of a base frame for a 3 MW turbo compressor

Eser Yarar[1], Murat Makaracı[1,*], Şaban Yılmaz[1,2], Ömer Apsar[2], Esra Kan[2,3]

[1] Mechanical Engineering Department, Engineering Faculty, Kocaeli University, Kocaeli 41001, Turkey

[2] IHI Dalgakıran Company, Kocaeli 41455, Turkey

[3] Mechanical Engineering Department, Engineering Faculty, Yıldız Technical University, İstanbul 34349, Turkey

* Corresponding author: Murat Makaracı, mmakaraci@kocaeli.edu.tr

Abstract: This study focuses on the design and analysis of a base frame for a 3 MW turbo compressor, aiming to develop a robust and reliable structural framework. The design process included comprehensive simulations, incorporating static stress-strain and dynamic vibration analyses to assess the base frame' performance under operational conditions. The static analysis evaluated the total deformation and strain behavior of the base frame, ensuring it can withstand the maximum load without yielding or excessive deformation. Dynamic vibration analysis was performed to identify the natural frequencies and potential resonance issues, minimizing the risk of vibrations that could compromise operational stability. Results from the static analysis revealed that the initial design exhibited a maximum total deformation of 0.24 mm, which was reduced to 0.09 mm in the final design—a 62.5% improvement. Elastic strain values were within safe operational limits for both designs. The effective mass ratio analysis showed significant results at frequencies close to 0 Hz, with negligible impact across the operating frequency range. Based on these analyses, an optimized base frame model was developed, meeting the design criteria for mechanical strength and vibrational stability. The results highlight the importance of integrating deformation, strain, and vibration assessments in the structural design of heavy-duty turbo compressor base frame, contributing to enhanced durability and performance.

Keywords: turbo compressor base frame; finite element method; stress-strain analysis; vibration analysis; structural optimization; dynamic simulation

1. Introduction

Turbo compressors are necessary components in various industrial applications, such as power generation, chemical processing, and oil and gas industries. These machines operate under high mechanical stress and rotational speeds, making the design of their supporting structures essential to ensuring safe and efficient performance [1]. Among the various parts of a turbo compressor, the base frame plays an important role in maintaining structural integrity, mitigating vibrations, and supporting operational loads [2,3]. As compressors are designed to handle substantial power outputs, particularly in large-scale applications like a heavy-duty system, their base frame must be engineered to endure significant static and dynamic forces. The primary challenge in designing a base frame for a high-capacity turbo compressor is ensuring its ability to withstand the stresses and strains induced by both operational loads and dynamic effects, such as vibrations. The presence of vibrations, especially resonant frequencies, can lead to excessive wear, fatigue failure, and performance degradation. Thus, it is crucial to conduct both static stress-strain analysis and dynamic

vibration assessments during the design phase to predict and prevent potential issues, ensuring the longevity and reliability of the system.

The design of a heavy-duty compressor base frame involves careful attention to various factors to ensure its performance and durability under operational conditions. Modal analysis plays an important role in understanding the dynamic behavior of the base frame, especially concerning vibration characteristics [4]. Compressors experience significant forces and operational stresses, making both static and modal vibration analyses essential to evaluate the base frame's ability to handle these loads without affecting its functionality. Modal analysis identifies the natural frequencies and mode shapes of the base frame, which helps to detect resonance conditions that could lead to mechanical failure or reduced performance [5]. Additionally, the effective mass ratio, a parameter obtained from modal analysis, quantifies the portion of the base frame mass involved in vibration modes, affecting the base frame's dynamic response [6,7]. By incorporating these analyses, the base frame can be designed to maintain both static strength and dynamic stability, enhancing the overall efficiency and longevity of the compressor system. The effective mass ratio is an important parameter in modal analysis as it determines the portion of the structure's total mass that participates in each vibration mode. This ratio is particularly significant because it directly affects the dynamic response of the base frame during operation. A higher effective mass in a given mode indicates that a larger portion of the base frame is involved in that vibration, increasing the likelihood of resonance at the corresponding frequencies. Resonance can lead to excessive vibrations, potentially causing damage, reducing structural integrity, or leading to operational inefficiencies [8]. Therefore, designers should examine the effective mass ratio to identify the most significant vibration modes and ensure that the base frame is adjusted to avoid resonance with these modes within its operational frequency range. While the literature extensively addresses the design and structural analysis of compressor components, it is important to integrate both static and dynamic simulations to optimize base frame designs. Furthermore, the high-power output of large turbo compressors presents unique challenges in terms of load distribution and material selection, making this a critical area of study. Jadhav and Dhanvijay [9] investigated the design of compressor base frames for high-speed reciprocating compressors, focusing on their performance under dynamic loading conditions. Finite element analysis (FEA) was employed to identify critical stress regions and evaluate the frame's capacity to withstand operational loads. Harmonic response analysis was conducted to assess vibrations induced by acceleration, with results benchmarked against standard data. The study confirmed that the base frame design complied with performance and durability requirements. According to ISO 10186 Part-6 [10–12], the vibration levels at the compressor bed were within acceptable limits, not exceeding 17.88 mm/s. Additionally, vibration isolation measures were incorporated into the existing design to enhance operational stability. Salunkhe et al. [13] addressed the growing demand for lightweight structural materials in industrial applications to enhance product efficiency and reliability. Their study focused on optimizing the base frame of a newly launched series of Multi Compressor Packs by Emerson, showcased at the Accrex Exhibition-2015. The initial base frame design was revised, and the layout was finalized from a structural perspective. A CAD model of the redesigned

frame was developed, followed by free vibration and static analyses using FEA software. The results determined the suitability of the base frame for operational frequency conditions. Further optimization was performed to ensure structural robustness. Experimental validation of the numerical findings was planned using an FFT analyzer on the newly manufactured frame. The primary objective of the study was to develop a base frame capable of withstanding the entire frequency range associated with the product's operation. Sherje and Agrawal [14] conducted a design and analysis study of an existing base frame to address its over-engineered nature, aiming to reduce weight and cost. The initial analysis revealed that the frame's excessive reliability resulted in unnecessary material use, prompting optimization for efficiency. Static and dynamic loads were evaluated, and the material, Fe 410 steel with a minimum tensile strength of 410 N/mm^2, was analyzed. The natural frequency of the base frame was determined both analytically and experimentally. Stiffness values for maximum and minimum deformation were used to calculate natural frequencies, with the average of these values considered as the final frequency. Experimental testing involved exciting the frame at four points using a hammer, and response data were analyzed using an FFT analyzer, resulting in Frequency vs. Acceleration plots. These experimental results were compared with finite element analysis (FEA) conducted in Ansys, revealing a discrepancy of less than 10%, thereby validating the accuracy of the computational model. A free vibration analysis identified 15 modes, with the initial six being rigid body modes and the remaining classified as normal modes. Importantly, none of the identified natural frequencies overlapped with the operational frequency of the compressor, effectively mitigating the risk of resonance. Kachare and Wankhede [15] developed a skid structure using conventional CAD practices, followed by static analysis using FEA software. The design aimed to minimize weight while ensuring structural integrity. The skid was required to control motion under load conditions, functioning similarly to a shock absorber, particularly during startup. To address high-frequency, small-amplitude excitations, a compliant but highly damped mount was integrated to achieve vibration isolation. In contrast to other approaches, the static analysis directly transferred forces from the load footprints to the main structural beams. This method improved load modeling accuracy by ensuring the primary beams bore the majority of the weight. Shear force and bending moment diagrams were generated for beams subjected to significant loads. Modal analysis revealed natural frequencies ranging from 99.335 Hz to 158.11 Hz, while the compressor's operational frequency (1450 RPM or 24.66 Hz) remained well below this range, effectively avoiding resonance. The maximum stress and deformation levels remained within permissible limits, confirming the design's safety and performance.

The design and analysis of base frames for large-scale turbo compressors remain an underexplored area in the existing body of research. While previous studies [16–20] have extensively addressed the structural and dynamic performance of smaller-scale systems, there is a notable lack of focus on the challenges associated with the design of base frames for turbo compressors operating at high power levels, such as 3 MW, and at significantly different rotational speeds for interconnected components. These challenges include managing the combined static and dynamic loads from critical components like the gearbox, electric motor, and additional subsystems such

as heat exchangers and cooling units, which collectively influence the structural integrity and vibration performance of the frame. The base frame design presented in this study was developed based on existing design knowledge and engineering practices. The initial design was created with the objective of providing sufficient structural support for the compressor and its auxiliary systems. To ensure its viability and performance under real-world conditions, the design was subjected to detailed FEA. Both static and dynamic vibration analyses were carried out to assess the base frame' behavior under operational conditions. The results of these analyses revealed critical areas of concern related to stress distribution, potential resonance frequencies, and dynamic deflections. Informed by the results from the FEA simulations, the final design was optimized to meet all required specifications, addressing both static load-bearing and dynamic vibration constraints. This iterative process ensured that the final base frame design met the necessary criteria for strength, durability, and vibrational stability, while also accommodating the additional components and ensuring effective load distribution.

2. The finite element model

Figure 1 shows the base frame model for both the initial design and the final design. The preliminary design of the turbo compressor base frame was developed to accommodate the specified components and ensure optimal structural integrity under operational conditions. The primary components supported by the base frame include the electric motor (10,064 kg), oil tank (1400 kg), gearbox (7200 kg), gas cooler (2770 kg), and control panel (75 kg). Each component serves a critical function in the compressor system, such as the electric motor providing mechanical motion, the gearbox ensuring proper speed regulation, and the gas cooler controlling the temperature of compressed air. more detailed specifications and boundary conditions are given in **Table 1**.
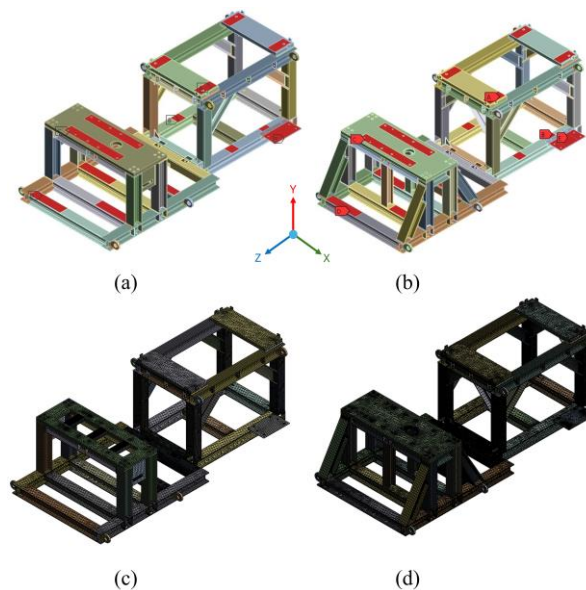

(a)   (b)

(c)   (d)

Figure 1. 3D model of base frames, **(a)** initial design; **(b)** final design; **(c)** mesh structure of initial design; **(d)** mesh structure of final design.

Table 1. Loads and properties of the base frame.

Component Name	Function	Weight (kg)	Mounting Location	Key Features
Electric Motor	The electric motor is the power source that provides the mechanical motion for the compressor.	10,064	A	Operates at 3000 rpm, high power
Oil Tank	The oil tank stores the oil in the system and ensures it circulates at the correct pressure.	1400	B	
Gear Box	The gearbox is a component that ensures the moving parts of the compressor operate at the correct speed.	7200	C	1st, 2nd impeller rotation speed 18930 rpm. 3rd, 4th 25438 rpm
Gas Cooler	The gas cooler, at the end of each stage, cools the compressed air to control the temperature rise.	2770	D	
Control Panel	The control panel is used to monitor the compressor's operating condition, make adjustments, and manage its settings.	75	E	

Structural steel was selected as the material for the base frame, offering a suitable balance of mechanical strength, stiffness, and durability under the operational loads of a 3 MW turbo compressor system. The material used in this study is assumed to follow a linear elastic constitutive relation, meaning that the material behaves in a manner where stress is directly proportional to strain within the elastic limit. The frame design incorporated bonded connections at critical joints to ensure structural rigidity and effective load transfer during operation. A tetrahedral mesh was chosen for finite element analysis (FEA), with a minimum element size of 35 mm to provide adequate resolution while maintaining computational efficiency. The meshing process resulted in 1,670,518 nodes and 920,843 elements for the initial design, and 1,727,503 nodes and 930,469 elements for the final optimized design. For static analysis, a gravitational load (9.81 m/s^2) was uniformly applied to the model to simulate the effects of self-weight. Fixed boundary conditions were imposed at the ground contact zones of the base frame to replicate its real-world constraints. These zones were defined based on the actual mounting locations and contact areas of the frame with the foundation. In the modal analysis, the first 600 modes were evaluated to identify potential resonance frequencies. The analysis specifically considered the operational frequencies of the system, including the 50 Hz working frequency of the electric motor and the ± 25% range around this frequency, as these are critical for ensuring that resonance effects are avoided. Additionally, the mode shapes were closely examined at mounting regions for the gearbox and electric motor to assess localized vibrational behavior.

3. Results and discussion

The deformation distributions obtained after the analyzes are given in **Figure 2**. The initial design of the base frame showed a maximum deformation of 0.24 mm. This value is not within acceptable limits and indicated that there were areas where the structural performance could be improved to reduce deflection and enhance the base frame's ability to withstand the applied forces. After optimizing the design based on the results of the static and dynamic simulations, the final design showed a significant reduction in deformation, with the maximum displacement reduced to 0.09 mm. This improvement indicates a stiffer structure that can better withstand the forces generated

by the high-speed rotation of the compressor shaft and the electric motor. The reduction in deformation not only ensures that the base frame maintains its shape under load but also increases its resistance to fatigue, as lower deformation reduces the strain on the material over time. The reduction in maximum deformation by 62.5% from the initial to the final design demonstrates the effectiveness of the optimization process. The revised design, with reinforcement in critical areas and adjustments to material properties or geometry, achieved a more uniform distribution of forces, reducing localized stress concentrations that previously contributed to higher deformation. This change ensures that the base frame performs efficiently under the operational conditions of the 3 MW turbo compressor, reducing the risk of structural failure and extending the system's lifespan.
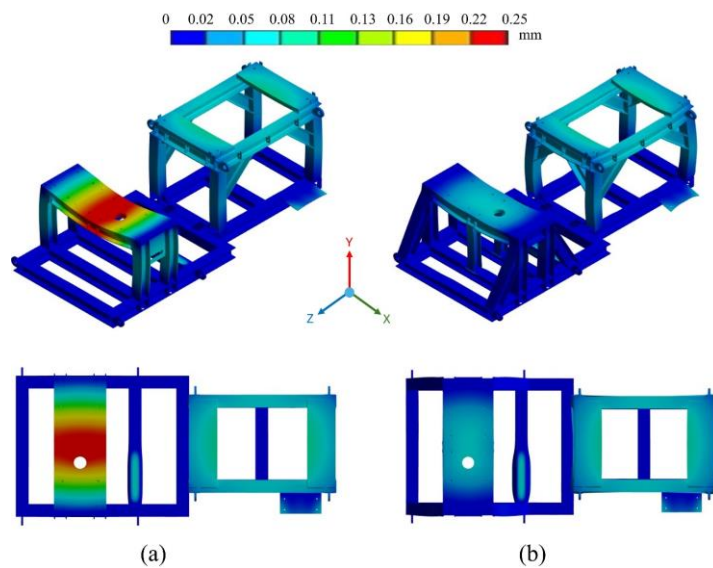

Figure 2. Total deformations, **(a)** initial design; **(b)** final design.

Figures 3 and **4** show the normal elastic strain distributions in the Y and X directions. The elastic strain values obtained in both the initial and final designs suggest that the base frame remains well within the acceptable limits of material performance, with no indication of any risk of material failure or yielding. Elastic strain, by definition, occurs within the elastic range of the material, meaning that the material will return to its original shape once the applied loads are removed, as long as the strain remains below the material's yield point.

In the initial design, the maximum elastic strain in the Y-direction was 10.6×10^{-5} and the minimum strain was -58.7×10^{-5}, while in the X-direction, the maximum strain was 24.1×10^{-5} and the minimum strain was -17.7×10^{-5}. These strain values, though indicating some level of deformation, are well within the elastic limits of typical materials used in base frame construction. They are not indicative of any immediate risk of material failure or permanent deformation, suggesting that the design can withstand the applied forces without compromising the material's integrity. In the final design, the maximum elastic strain in the Y-direction decreased to 9.72×10^{-5} and the minimum strain improved to -62.5×10^{-5}, while in the X-direction, the maximum strain reduced to 14.3×10^{-5} and the minimum strain improved to -17.6×10^{-5}. These reductions indicate that the optimization process led to a more efficient

distribution of forces and a slight decrease in overall material deformation. However, despite these improvements, the final strain values still remain within safe limits and do not suggest any dangerous level of deformation that could lead to material failure. The reduction in strain values after optimization demonstrates a more balanced and efficient force distribution, but it should be noted that the initial strain values were already within acceptable limits. Thus, while the optimization process improved the design, the initial design was not at risk of failure or significant deformation. The improvements serve more to enhance the structural efficiency and longevity of the base frame rather than to address critical safety concerns.
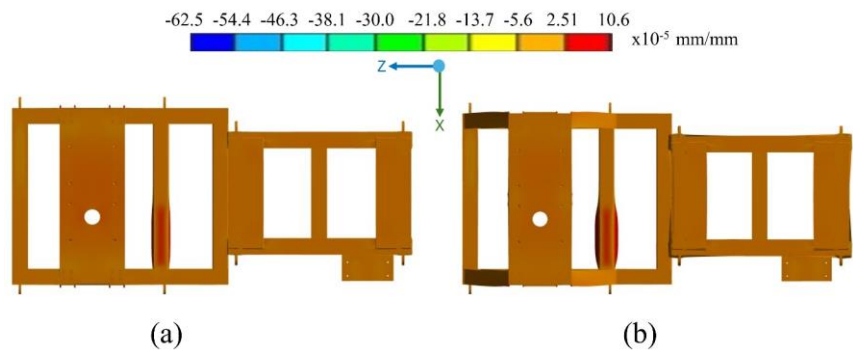

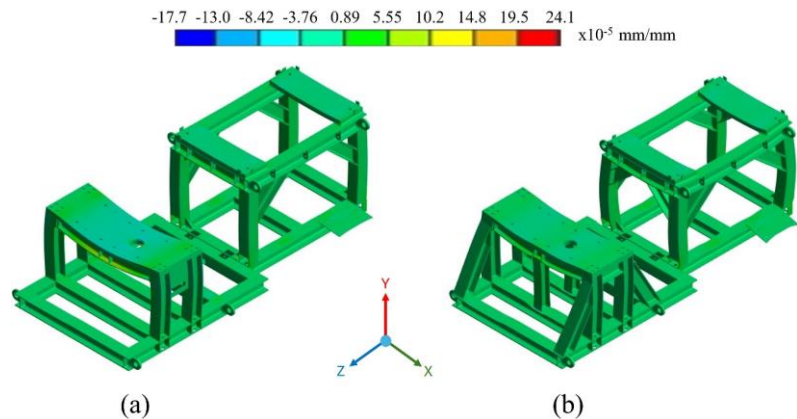**Figure 3.** Normal elastic strain Y axis, **(a)** initial design; **(b)** final design.

Figure 4. Normal elastic strain X axis, **(a)** initial design; **(b)** final design.

Table 2 shows the effective mass ratio obtained for the initial design. The table was created for modes with ratio values greater than at least 4 percent. In the X-direction, modes 1 and 3 dominate the displacement behavior, with a clear contribution from both modes (39.49% and 29.45% of the total modal mass). The initial mode with a frequency of 10.36 Hz shows a significant displacement, indicating that the base frame experiences notable lateral movement under this frequency. The second mode, with a higher frequency of 14.47 Hz, still contributes substantially to the deformation in the X-direction but with a slightly lower displacement. These values suggest that the base frame may experience significant lateral motion, potentially influencing the structural stability under operational conditions. In the Z-direction, mode 4 with a frequency of 16.36 Hz shows the highest displacement (11.61) and accounts for the greatest modal mass contribution (39.65%). This suggests that side to side motion at this frequency will have a significant impact on the base frame. Mode 5, with a higher

frequency of 23.55 Hz, also contributes substantially to vertical motion but with a slightly reduced displacement. Higher frequency modes such as Mode 10 and Mode 21 have relatively small contributions to Z-direction displacement, indicating that their influence on the side-to-side motion of the base frame is limited. In the Y-direction, mode 8 and mode 13 are the main contributors to displacement. Mode 8, with a frequency of 34.59 Hz, contributes 25.98% of the modal mass, and mode 13 with a frequency of 60.84 Hz shows an even higher contribution of 29.8%. These modes indicate that the base frame experiences noticeable vertical motion at these frequencies, which could affect the stability of the structure, especially during high-speed operation when these frequencies might be excited. **Figures 5** and **6** show the mode shapes obtained for these critical modes.

Table 2. Effective mass ratio of initial design.

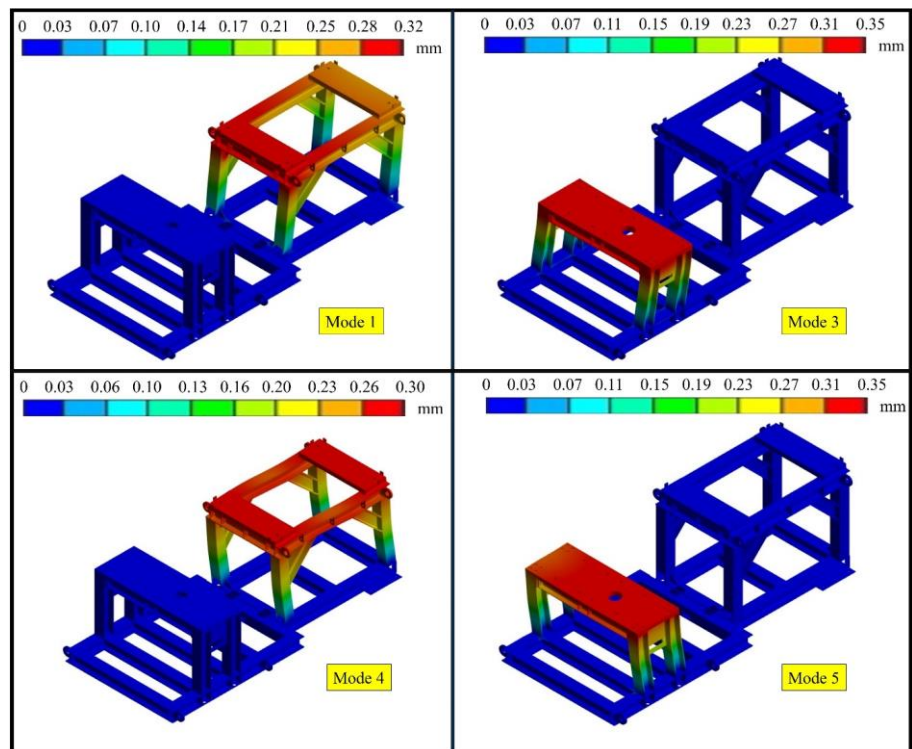| Mode | Frequency (Hz) | Modal Mass (kg) | Effective mass | | | | | |
			X-dir	Ratio%	Y-dir	Ratio%	Z-dir	Ratio%
1	10.36	9.6	11.56	39.49	1.97×10^{-7}	0	1.91×10^{-6}	0
3	14.47	8.1	8.619	29.45	8.97×10^{-5}	0	2.09×10^{-8}	0
4	16.36	11	2.17×10^{-7}	0	5.41×10^{-7}	0	11.61	39.65
5	23.55	8.1	1.15×10^{-6}	0	3.01×10^{-5}	0	8.683	29.67
8	34.59	5.3	3.45×10^{-5}	0	7.605	25.98	4.68×10^{-6}	0
10	36.22	1.5	1.87×10^{-5}	0	8.17×10^{-5}	0	1.71	5.84
13	60.84	3.8	1.13×10^{-6}	0	8.723	29.8	2.38×10^{-5}	0
21	71.02	0.7	1.60×10^{-5}	0	2.21×10^{-5}	0	1.255	4.29
sum			28.12	96.07	26.81	91.61	28.23	96.43

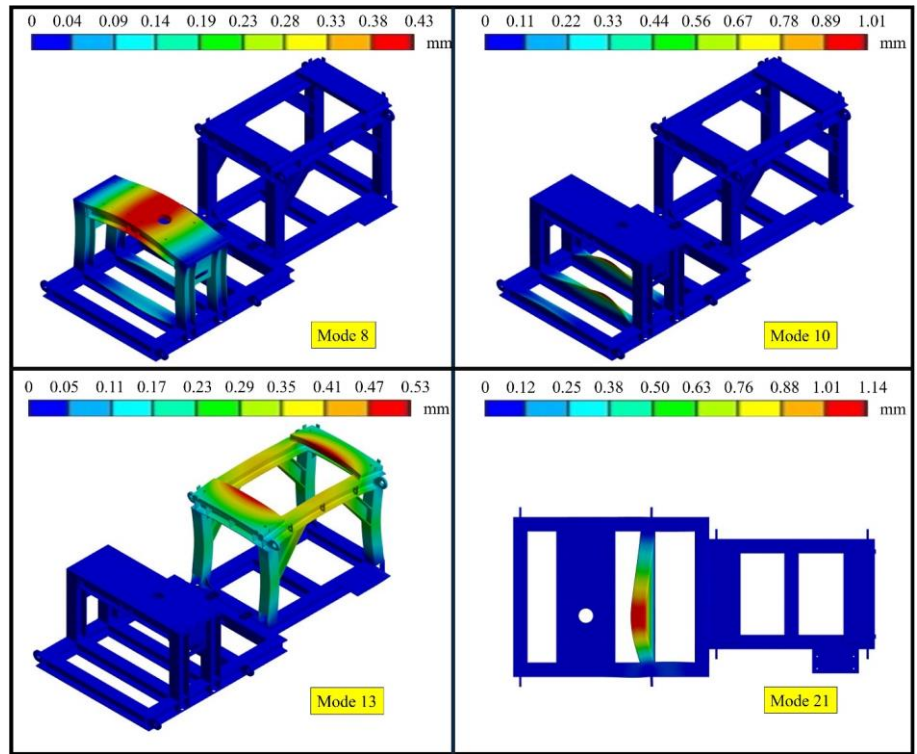**Figure 5.** Mode shapes of initial design 1.

Figure 6. Mode shapes of initial design 2.

Table 3. Effective mass ratio of final design.

Mode	Frequency (Hz)	Modal Mass (kg)	Effective mass					
			X-dir	Ratio%	Y-dir	Ratio%	Z-dir	Ratio%
1	14.21	9.679	11.68	39.33	7.66×10^{-7}	0	1.17×10^{-5}	0
3	16.34	10.97	3.50×10^{-6}	0	4.72×10^{-6}	0	11.7	39.38
4	18.12	8.178	8.85	29.79	1.33×10^{-4}	0	2.19×10^{-4}	0
8	45.01	1.279	1.20×10^{-6}	0	1.10×10^{-4}	0	3.489	11.74
9	49.67	8.09	1.23×10^{-7}	0	3.26×10^{-4}	0	7.191	24.21
26	86.85	1.14	8.98×10^{-6}	0	3.038	10.23	7.69×10^{-5}	0
sum			28.55	96.11	27	90.88	28.66	96.48

Table 3 shows the effective mass ratio obtained for the final design. The table was created for modes with ratio values greater than at least 6%. The modal analysis results for the final base frame design illustrate its dynamic characteristics in response to vibrations across different directions. In the X-direction, mode 1 at a frequency of 14.21 Hz has the highest modal mass contribution, accounting for 39.33% of the total modal response. The displacement at this frequency is 11.68, indicating that lateral movement is prominent in this mode. Mode 4, with a frequency of 18.12 Hz, contributes 29.79% to the modal response, demonstrating that the base frame continues to show significant lateral behavior at slightly higher frequencies. In the Z-direction, mode 3 at 16.34 Hz dominates the vertical response with a modal mass contribution of 39.38% and a displacement of 11.7, making it the most significant mode for vertical motion. At higher frequencies, modes 8 and 9, with frequencies of 45.01 Hz and 49.67 Hz respectively, show reduced modal contributions. However,

mode 9 still accounts for 24.21% of the response, indicating notable vertical behavior at this frequency. The Y-direction response is primarily influenced by mode 26 at a frequency of 86.85 Hz, with a modal mass contribution of 10.23% and a displacement of 3.038. Although the contribution is less significant compared to the dominant modes in the X and Z directions, it highlights the side-to-side motion at higher frequencies.
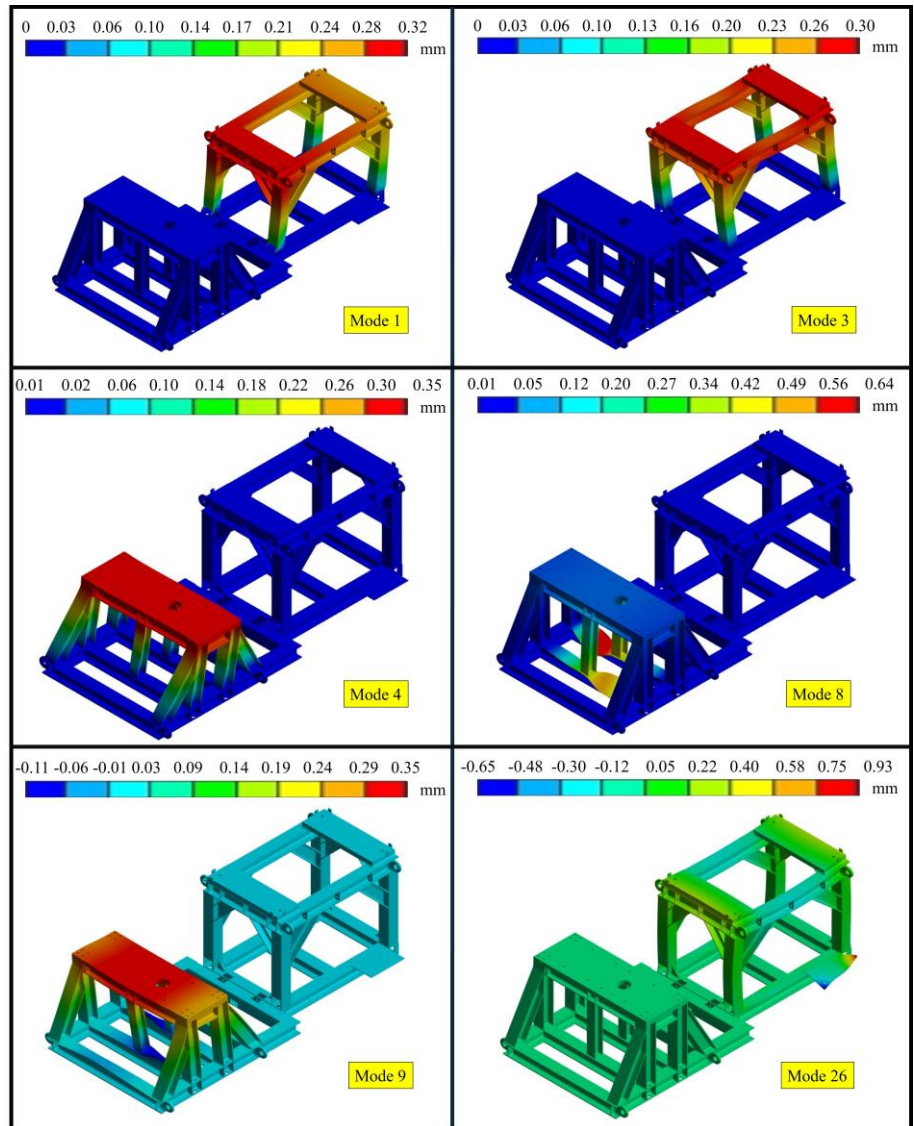

Figure 7. Mode shapes of final design.

The mode shapes depicted in **Figure 7** provide information on the dynamic behavior of the final base frame design, particularly regarding the gearbox and electric motor regions. The section of the base frame responsible for transmitting rotational drive from the gearbox demonstrates no issues within its operational frequency range, as evidenced by the Effective Modal Mass Ratio analysis. The modes contributing to this region's response indicate stable performance, ensuring that the dynamic loads from the gearbox remain within acceptable limits. Modes 8 and 9, occurring at 45.01 Hz and 49.67 Hz respectively, fall within the resonance frequency range of the electric motor, which operates at 50 Hz with a ± 25% tolerance (i.e., 37.5 Hz to 62.5 Hz). This

overlap initially suggests potential resonance concerns. However, upon examining the mode shapes of these modes, the vibration amplitudes in the region where the electric motor is mounted are observed to be nearly zero. This indicates that the motor mounting area remains dynamically stable, even at frequencies close to resonance, thereby minimizing the risk of excessive vibration or performance degradation. As a result of the optimization process, the final base frame design achieves a maximum static deformation below the acceptable limit of 0.1 mm, ensuring structural stability under load. Additionally, considering the operational frequencies of the system, the design aligns with industry standards for vibration performance. The modal analysis confirms that the critical regions of the base frame, including the gearbox and electric motor mounting areas, exhibit no significant resonance-related issues. Specifically, while certain modes fall within the resonance frequency range of the electric motor, the negligible vibration amplitudes in these regions demonstrate that the base frame effectively minimizes the impact of potential resonance.

4. Conclusion

This study successfully designed and optimized a turbo compressor base frame capable of supporting critical components under challenging operational conditions. The initial design underwent a comprehensive evaluation through finite element analysis, including static and modal assessments, to identify areas for improvement. Static analysis indicated that the initial design exhibited a maximum total deformation of 0.24 mm, which was reduced to 0.09 mm in the optimized design, achieving a 62.5% improvement in structural performance. Elastic strain values remained within safe operational limits for both designs, ensuring material reliability and resistance to fatigue. Modal analysis shows that resonance effects will not adversely affect dynamic performance. This finding confirms that the optimized design effectively avoids resonance, ensuring dynamic stability during high-speed operations. The final design incorporates improvements such as reduced local stress concentrations and enhanced stiffness, contributing to its ability to withstand the forces generated by the compressor's components, including an electric motor operating at 3000 rpm and a compressor impeller's at 18,930 rpm and 35,438 rpm. The iterative design approach, supported by advanced simulation techniques, has resulted in a base frame that meets the structural and operational requirements of a 3 MW turbo compressor.

References

1. Whitfield A, Doyle MDC, Firth MR. Design and performance of a high-pressure ratio turbocharger compressor Part 2: Experimental performance. Proc. Inst. Mech. Eng. Part A J. Power. Energy. 1993; 207: 125–131. doi: 10.1243/PIME_PROC_1993_207_021_02

2. Giampaolo T. Compressor Handbook: Principles and Practice. Fairmont Press; 2010.

3. Hong DK, Jeong YH, Woo BC, Kim TH. Electric-mechanical performance analysis of high speed motor for electric turbo charger. Int. J. Appl. Electromagn. Mech. 2018; 57: 125–133. doi: 10.3233/jae-182303

4. Shejal PP, Desai AD. Pulsation and Vibration Study of Reciprocating Compressor According to API 618 5th Edition. Ijmer. 2014; 4: 1–23.

5. Bonello P. Transient modal analysis of the non-linear dynamics of a turbocharger on floating ring bearings. Proc. Inst. Mech. Eng. Part J J. Eng. Tribol. 2009; 223: 79–93. doi: 10.1243/13506501JET436

6. Spears RE, Jensen SR. Approach for selection of rayleigh damping parameters used for time history analysis. J. Press. Vessel Technol. 2012; 134: 061801. doi: 10.1115/1.4006855

7. Weng G, Hui Y, Cao J. Time-varying mechanism of fluid-structure interaction vibration effects and dynamic characteristics of the cross-over pipeline when the medium flows. Structures. 2023; 57: 105151. doi: 10.1016/j.istruc.2023.105151

8. Makaraci, M. A multi-objective design optimization procedure for a general control system. In: Proceedings of the Seventh International Conference and Exposition on Engineering, Construction, Operations and Business in Space; 27 February–2 March 2000; Albuquerque, NM, USA. pp. 377–383.

9. Jadhav KD, Dhanvijay MR. Design and Standardization of Base Frame & Ant Vibration Mounts for Balanced Opposed Piston Air Compressor. Int. J. Appl. Res. Mech. Eng. 2012; 2(2); 100–107. doi: 10.47893/IJARME.2012.1071

10. ISO. ISO 10816:2014-Mechanical vibration—Evaluation of machine vibration by measurements on non-rotating parts. ISO; 2014.

11. Centomo S, Dall'ora N, Fummi F. The Design of a Digital-Twin for Predictive Maintenance. In: Proceedings of the 25th IEEE International Conference on Emerging Technologies and Factory Automation; 08–11 September 2020; Vienna, Austria. pp. 1781–1788.

12. Dambrauskas K, Vanagas J, Zimnickas T, et al. Induction motor's bearing condition motoring and diagnosis applying cloud services and artificial neural networks. In: Proceedings of the 7th IEEE Workshop on Advances in Information, Electronic and Electrical Engineering (AIEEE); 15–16 November 2019; Liepaja, Latvia. pp. 8–12.

13. Salunkhe PA, Kulkarni G, Begad M. Static and Free Vibration Analysis of Multi-Compressor Packs Base. International Journal of Advance Research and Innovative Ideas in Education. 2016; 2(4): 161–171.

14. Agrawal S, Sherje N, Umbarkar A. Design and Analysis of Compressor Base Frame for Weight Reduction. SSRN Electron. J. 2019. doi: 10.2139/ssrn.3350911

15. Kachare PP, Wankhede AR, Momale VC. Basic Optimization of Compressor Frame. International Journal of Emerging Technologies and Innovative Research. 2019; 6: 113–116.

16. Ahmed AA, Fattah MY, Mohsen MK. Effect of frame foundation geometry on the dynamic response of high-speed turbo machine foundations. Heliyon. 2025; 11(1): e41050. doi: 10.1016/j.heliyon.2024.e41050

17. Khamari DS, Kumar J, Behera SK. Rotordynamic analysis of a complex high-speed rotor. Materials Today: Proceedings. 2023; 90: 299–304. doi: 10.1016/j.matpr.2023.07.322

18. Fakhari SM, Hassen MB, Mrad H. Optimizing the operation safety and performance of an axial compressor using fluid-structure coupling and high-performance computing. Results in Engineering. 2023; 18: 101061. doi: 10.1016/j.rineng.2023.101061

19. Shao J, Wu J, Cheng Y. Nonlinear dynamic characteristics of a power-turbine rotor system with branching structure. International Journal of Non-Linear Mechanics. 2023; 148: 104297. doi: 10.1016/j.ijnonlinmec.2022.104297

20. Nan G, Yao X, Yang S, et al. Vibrational responses and fatigue life of dynamic blades for compressor in gas turbines. Engineering Failure Analysis. 2024; 156: 107827. doi: 10.1016/j.engfailanal.2023.107827